Environ. Sci. Technol. **2006**, *40,* 1286−1299

Modeling Ozone and Aerosol Formation and Transport in the Pacific Northwest with the Community Multi-Scale Air Quality (CMAQ) Modeling System

SUSAN M. O'NEILL,*,† BRIAN K. LAMB,‡ JACK CHEN,‡ CANDIS CLAIBORN,‡ DENNIS FINN,‡ SALLY OTTERSON,§ CRISTIANA FIGUEROA,§ CLINT BOWMAN,§ MIKE BOYER,§ ROB WILSON,|| JEFF ARNOLD,|| STEVEN AALBERS,⊥ JEFFREY STOCUM,⊥ CHRISTOPHER SWAB,⊥ MATT STOLL,@ MIKE DUBOIS,@ AND MARY ANDERSON@

Pacific Wildland Fire Sciences Laboratory, U.S. Department of Agriculture Forest Service, 400 North 34th Street, Suite 201, Seattle, Washington 98103, Department of Civil and Environmental Engineering, Washington State University, Pullman, Washington 99164-2910, Washington State Department of Ecology, P.O. Box 47600, Olympia, Washington 98504-7600, U.S. Environmental Protection Agency Region 10, 1200 Sixth Avenue (OEA-095), Seattle, Washington 98101-1128, Oregon Department of Environmental Quality, 811 Southwest Sixth Avenue, Portland, Oregon 97204-1390, Idaho Department of Environmental Quality, 1410 North Hilton, Boise, Idaho 83706-1255

The Community Multi-Scale Air Quality (CMAQ) modeling system was used to investigate ozone and aerosol concentrations in the Pacific Northwest (PNW) during hot summertime conditions during July 1−15, 1996. Two emission inventories (EI) were developed: emissions for the first EI were based upon the National Emission Trend 1996 (NET96) database and the BEIS2 biogenic emission model, and emissions for the second EI were developed through a "bottom up" approach that included biogenic emissions obtained from the GLOBEIS model. The two simulations showed that elevated $PM_{2.5}$ concentrations occurred near and downwind of the Interstate-5 corridor along the foothills of the Cascade Mountains and in forested areas of central Idaho. The relative contributions of organic and inorganic aerosols varied by region, but generally organic aerosols constituted the largest fraction of $PM_{2.5}$. In wilderness areas near the I-5 corridor, organic carbon from anthropogenic sources contributed approximately 50% of the total organic carbon with the remainder from biogenic precursors, while in wilderness areas in Idaho, biogenic organic carbon accounted for 80% of the total organic aerosol. Regional analysis of the secondary organic aerosol formation in the Columbia River Gorge, Central Idaho, and the Olympics/Puget Sound showed that the production rate of secondary organic carbon depends on local terpene concentrations and the local oxidizing capacity of the atmosphere, which was strongly influenced by anthropogenic emissions. Comparison with observations from 12 IMPROVE sites and 21 ozone monitoring sites showed that results from the two EI simulations generally bracketed the average observed PM parameters and that errors calculated for the model results were within acceptable bounds. Analysis across all statistical parameters indicated that the NW-AIRQUEST EI solution performed better at predicting $PM_{2.5}$, PM_1, and β_{ext} even though organic carbon PM was over-predicted, and the NET96 EI solution performed better with regard to the inorganic aerosols. For the NW-AIRQUEST EI solution, the normalized bias was 30% and the normalized absolute error was 49% for $PM_{2.5}$ mass. The NW-AIRQUEST solution slightly overestimated peak hourly ozone downwind of urban areas, while the NET96 solution slightly underestimated peak values, and both solutions over-predicted average O_3 concentrations across the domain by approximately 6 ppb.

1. Introduction

The Pacific Northwest (PNW) is home to a number of Class 1 wilderness areas and national parks where air quality and visibility issues are important. To improve our understanding of these issues, the CMAQ modeling system (*1*) was used to investigate ozone and aerosol concentrations and the visibility impacts of the aerosols in the PNW. This work was conducted through the Northwest International Air Quality Environment Science & Technology Consortium (NW-AIRQUEST; http://www.nwairquest.wsu.edu) to develop an understanding of the role of emissions and chemistry related to both regional fine particulate matter ($PM_{2.5}$) and ozone. The period of July 1−15, 1996 was selected for study because it included 4 days with elevated ozone concentrations along the Interstate-5 corridor, several of the Interagency Monitoring of PROtected Visual Environments (IMPROVE) sites in the domain measured visibility impairment, and because we had previously conducted a variety of modeling analyses of this ozone event (*2*−*5*). Malm et al. (*6*, *7*), in their analysis of data from the IMPROVE program, indicated that sulfate (SO_4), organic carbon (OC), and fine soil (SOIL) are the largest contributors to $PM_{2.5}$ mass in the Pacific Northwest, with organic aerosols contributing 40%−45% to light extinction in the PNW.

Two emission inventories (EI) were developed for this study. For the first EI, anthropogenic emissions were based on the National Emission Trend 1996 (NET96) database (*8*), and biogenic emissions were obtained from the Biogenic Emission Inventory System-2 (BEIS2, *9*) biogenic emissions model. For the second EI, anthropogenic emissions were developed from the "bottom up" by NW-AIRQUEST participants, and biogenic emissions were obtained from the Global Biosphere Emissions and Interactions System (GLOBEIS) biogenic emissions model (*10*), a canopy model similar to the current U.S. Environmental Protection Agency (U.S. EPA) regulatory model BEIS3 (*11*, *12*). This study thus explores the effects of uncertainties in aerosol precursor emissions by employing biogenic emissions obtained from

* Corresponding author phone: (503) 273-2438; fax: (503) 273-2401; e-mail: susan.oneill@por.usda.gov.
† Pacific Wildland Fire Sciences Laboratory. Now affiliated with USDA Natural Resources Conservation Service, Portland, Oregon.
‡ Washington State University.
§ Washington State Department of Ecology.
|| U.S. EPA Region 10.
⊥ Oregon Department of Environmental Quality.
@ Idaho Department of Environmental Quality.

10.1021/es048402k CCC: $33.50
Published on Web 01/19/2006

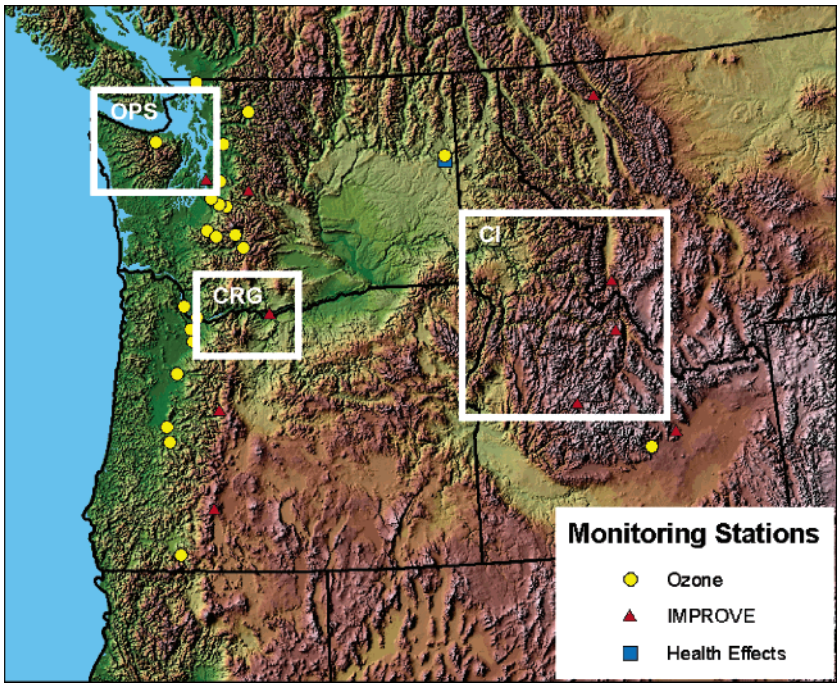

FIGURE 1. Terrain elevation and locations of the IMPROVE, Spokane Health Effects, and EPA AIRS ozone observation stations in operation during the July 3−16, 1996 period. Three regions are also identified: the Olympics/Puget Sound (OPS), the Columbia River Gorge (CRG), and Central Idaho (CI).

two biogenic emissions models and using two anthropogenic emission inventories with order of magnitude differences in ammonia emissions.

Previous studies have focused on the eastern United States (*13*, *14*) and California (*15*). The Pacific Northwest offers a different situation because of locally urbanized areas situated in a domain dominated by forests, mountains, and agricultural areas. The complex terrain of the Pacific Northwest is illustrated in Figure 1. Urbanization exists in the forested area between the coast and western ridge of the Cascade Mountains along the I-5 corridor. The east side of the Cascade Mountains is less heavily populated and lies in the rain shadow of the Cascades; thus, conditions are often hot and dry, especially in the summer months. The Columbia Plateau, spanning much of eastern Washington and south into Oregon, is an area rich in agriculture. The Rocky Mountains run north−south through Canada, Montana, and Idaho. The most populated area of Idaho is the Snake River valley, another active agricultural area, which loops through southern Idaho from east to west before turning north to the Oregon border.

The purpose of this paper is to present results describing ozone and aerosol formation in the PNW and to evaluate CMAQ v4.1 model performance using the two different EI for a period when ozone exceedances occurred and visibility impairment was measured. Model performance is analyzed for ozone, sulfate (SO_4), nitrate (NO_3), ammonium (NH_4), organic carbon, elemental carbon (EC), fine soil, PM_1 mass, and $PM_{2.5}$ mass, and visibility parameters (extinction coefficient (β_{ext}) and deciview).

2. Modeling System

Synoptic conditions for the 13-day period were characterized by a low pressure system off the Pacific coast for July 3−4, 1996. By July 5, 1996 a high pressure system was building off the coast of Washington and Canada which settled over British Columbia through July 14, 1996. Sunny conditions and above normal temperatures prevailed, especially through the July 11−14, 1996 period. These conditions were conducive to generating elevated ozone concentrations as discussed in Barna et al. (*2*). By July 15, 1996 a low-pressure system centered over eastern Washington and northern Idaho had been established.

TABLE 1. Performance Statistics of Index of Agreement (I), Mean Error (E), and Absolute Mean Error (|E|) Comparing the Three MM5 Solutions for the Period of July 1−16, 1996 with the 46 Surface Winds Observational Stations

	wind speed (m/s)			wind direction (deg)			temperature (°C)		
	I	E	|E|	I	E	|E|	I	E	|E|
July 1−6	0.59	−0.7	1.8	0.81	8.9	50	0.76	0.80	2.8
July 6−11	0.59	−1.0	1.9	0.87	6.6	48	0.82	0.33	2.8
July 11−16	0.70	−1.1	2.0	0.88	6.4	51	0.80	0.09	3.4

2.1 Meteorology. The Mesoscale Meteorological model, MM5 v3 (*16*), was applied to simulate the meteorological conditions for July 3−16, 1996. The actual modeled MM5 domain extends further north than shown in Figure 1. Thirty-seven vertical sigma levels were used, with the lowest sigma level approximately 40 m high. The 37 sigma levels were collapsed to 16 levels in the Meteorology−Chemistry Interface Processor (MCIP) v1, the CMAQ meteorological preprocessor. Emphasis was placed upon retaining resolution within the boundary layer.

Four-dimensional data assimilation (FDDA) analysis nudging was applied to both the 36-km domain and the 12-km domain for wind speed, temperature, and moisture fields from surface and upper air observational data. Model output was evaluated for wind speed, wind direction, and temperature at 46 surface station monitors and for wind speed and wind direction at 7 upper air stations. The 13-day period was split into three separate MM5 runs of 5.5 days each, accounting for a 12-h spin-up period and beginning on July 1 to allow for additional CMAQ spin-up. Table 1 summarizes the domain-wide statistical performance for each of the three periods. MM5 tended to under-predict the wind speed by 0.7−1.1 m/s while the absolute mean error for wind direction for all three periods was approximately 50 degrees. This

TABLE 2. Summary of Anthropogenic and Biogenic Emissions (Metric Tons per Day) Summed over the Entire Modeling Domain for the NW-AIRQUEST Emission Inventory and NET96 Emission Inventory (Vehicle Emissions Are Included in the Area Source Category)

	point sources		area sources		total anthropogenic emissions		biogenic sources		total emissions		percent anthropogenic (%)	
model species	NW-Airquest	Net 96	NW-Airquest	Net 96	NW-Airquest	Net 96	NW-Airquest	Net 96	NW-Airquest	Net 96	NW-Airquest	Net 96
acetic and higher acids	1	0	1	1	2		1625		626	1	0	100
aldehydes	2	1	27	20	28	21	1441		1470	21	2	100
alkanes w/$2.7 \times 10^{-13} >$ koh $< 3.4 \times 10^{-12}$	32	18	391	389	423	407	10526	901	10949	1308	4	31
alkanes w/$3.4 \times 10^{-12} >$ koh $< 6.8 \times 10^{-12}$	33	15	570	496	603	511			603	511	100	100
alkanes w/koh $> 6.8 \times 10^{-12}$	47	19	639	565	685	584			685	584	100	100
cresol	1	0	1	3	2	3			2	3	100	100
ethane	13	5	134	108	147	113	312		459	113	32	100
ethene	26	3	199	153	225	156	1295		1521	156	15	100
formaldehyde	7	4	44	38	51	42	2776		2826	42	2	100
internal olefins	11	4	146	111	157	115	4857	3965	5014	4080	3	3
isoprene							6569	11235	6569	111235	0	90
ketones	5	4	15	20	21	24	2433		2454	24	1	100
terminal olefins	19	3	115	74	134	77	8787		8921	77	2	100
terpenes							17883	4409	17883	4409	0	0
toluene	19	15	380	285	400	300			400	300	100	100
xylene	8	8	415	351	423	359			423	359	100	100
total VOC	225	100	3077	2613	3301	2713	57506	20509	60807	23222	5	12
ammonia	42	14	88	1005	130	1019			130	1019	100	100
carbon monoxide	2971	1024	26407	18371	29378	19395	8613		37991	19395	77	100
methane	70	24	1218	1158	1288	1182			1288	1182	100	100
nitric oxide	928	256	2029	1714	2957	1969	569	569	3525	2538	84	78
nitrogen dioxide	158	44	217	292	375	336			375	336	100	100
sulfur dioxide	1688	701	493	460	2181	1161			2181	1161	100	100
sulfuric acid	15	10	26	0	41	10			41	10	100	100
ammonium aerosol	1	0	2	2	3	2			3	2	100	100
coarse particulate	132	54	590	1756	722	1810			722	1810	100	100
elemental carbon	17	6	125	87	142	93			142	93	100	100
fine particulate	198	73	237	490	434	563			434	563	100	100
organic aerosol	51	17	223	208	273	225			273	225	100	100
sulfate aerosol	35	14	9	10	44	24			44	24	100	100

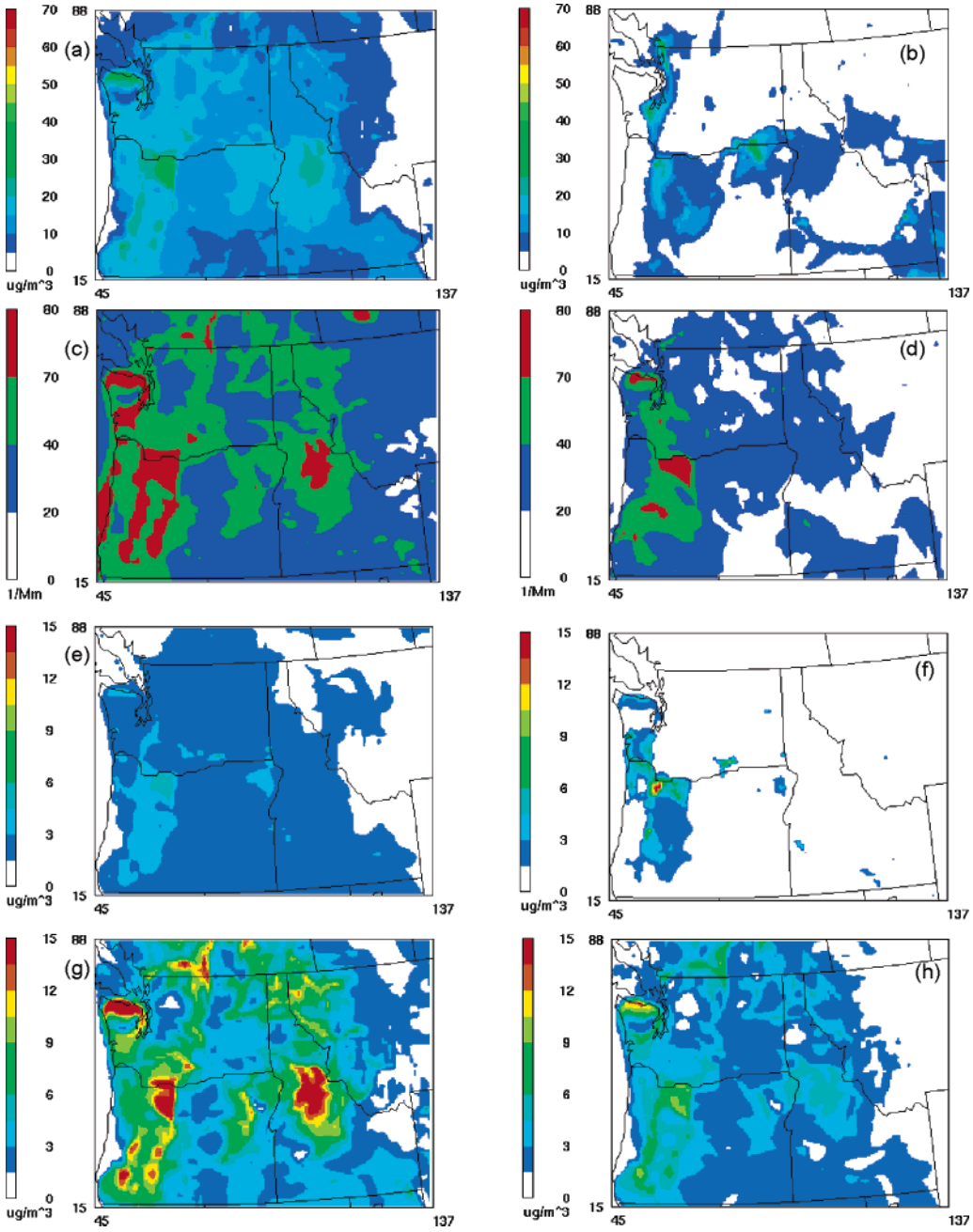

FIGURE 2. Aerosol concentrations for July 14, 1996, 7 a.m. PDT. (a) Total $PM_{2.5}$ from the NW-AIRQUEST EI. (b) Total $PM_{2.5}$ from the NET96 EI. (c) Reconstructed extinction coefficient predicted by the NW-AIRQUEST EI. (d) Reconstructed extinction coefficient predicted by the NET96 EI solution. (e) Inorganic aerosol concentrations from the NW-AIRQUEST EI. (f) Inorganic aerosol concentrations from the NET96 EI. (g) Organic aerosol concentrations from the NW-AIRQUEST EI. (h) Organic aerosol concentrations from the NET96 EI. The scale in (c) and (d) indicates $\beta_{ext} < 20$ = natural conditions, $\beta_{ext} > 20$ = noticeable impairment, $\beta_{ext} > 41$ = moderate degradation, and $\beta_{ext} > 70$ = severe degradation.

performance is similar to MM5 performance for the PNW in other studies (*3*, *17*).

2.2 Emission Inventories. The Sparse Matrix Operator Kernel Emissions (SMOKE) processor v1.4 (*18*) was used to prepare two emission inventories. Anthropogenic emissions for the first emission inventory were based upon a variation of the 1996 U.S. EPA National Emission Trends (NET96) database (*8*) that exists for North America at 36-km resolution. The second emission inventory was developed as a "bottom-up" approach with the NW-AIRQUEST stakeholders collaborating to better characterize emissions; this emission inventory will hereafter be referred to the NW-AIRQUEST emission inventory (*19*). As part of the NW-AIRQUEST effort, Canada provided a point source emission inventory.

The GLOBEIS biogenic emissions model (*10*) was used to obtain biogenic emissions for the NW-AIRQUEST EI, while the NET96 EI relies on the BEIS2 biogenic emission model (*9*). GLOBEIS relies on the BELD3 database (*20*) and BEIS3 (*11*, *12*) emission factors to estimate emissions of 18 terpene species, methyl-butenol (MBO), isoprene, and a lumped VOC category. BEIS2 outputs isoprene, terpene, alkanes, internal olefins, and NO.

Table 2 summarizes emissions for the 13-day period for point sources, area sources (which include vehicle emissions), and biogenic emissions. Several differences exist between the two inventories: Biogenic VOC emissions are 2.8 times higher in the NW-AIRQUEST EI than in the NET96 EI. Anthropogenic NH_3 emissions are 7.8 times higher in the

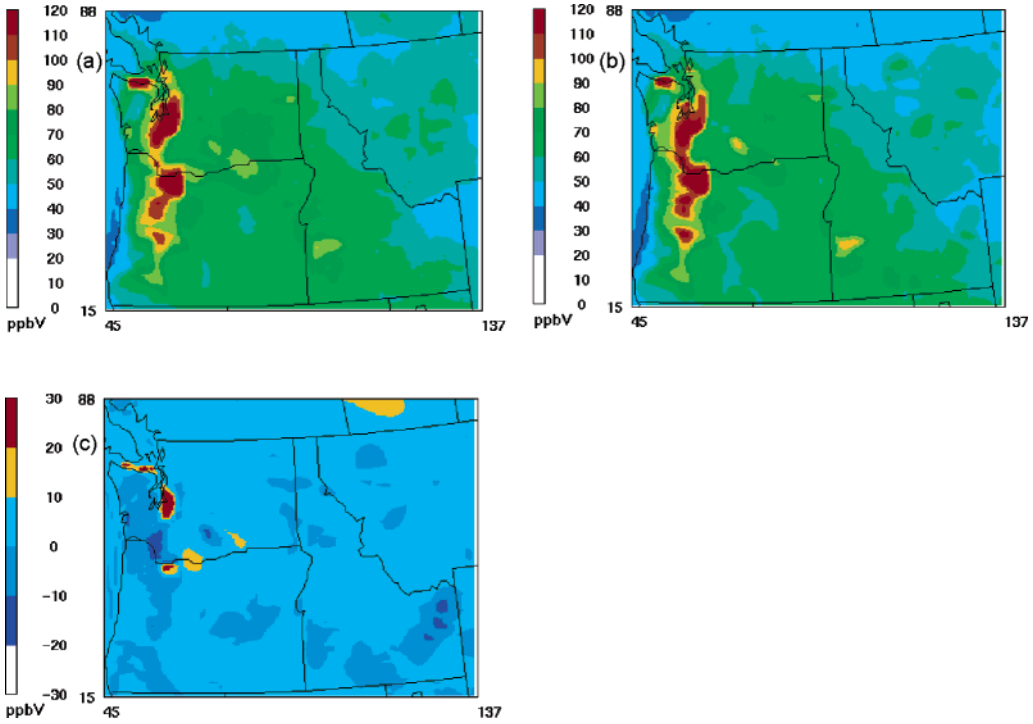

FIGURE 3. Ozone concentrations for July 14, 1996 at 4 p.m. PDT from the (a) NW-AIRQUEST EI solution and (b) NET96 EI solution, and (c) the difference between the two solutions obtained by subtracting the NET96 concentration field from the NW-AIRQUEST concentration field.

NET96 EI than in the NW-AIRQUEST EI. Anthropogenic SO_2 emissions are 1.9 times higher in the NW-AIRQUEST EI than in the NET96 EI. Total CO emissions are 2 times higher in the NW-AIRQUEST EI than in the NET96 EI.

These differences can be explained as follows. VOC emissions are larger in GLOBEIS than in BEIS2 due to changes in estimated emission factors (*21*). Methyl-butenol (MBO) was included in the GLOBEIS emissions and was not part of the BEIS2 emissions. MBO is known as the "isoprene of the west" and is ubiquitous in the northwest (*21*). MBO accounts for approximately 14% of the total VOCs. Terpene emissions were approximately 4 times higher with the BEIS3 and GLOBEIS emission factors than from BEIS2. Pressley et al. (*22*) measured monoterpene emissions from Douglas Fir and Hemlock in the Cascade Mountains of Washington State and found that the measured emission factors were 19% less than those in GLOBEIS and a factor of 3.3 higher than those in BEIS2. Point emission data were not provided for Canada in the NET96 EI but were obtained for the NW-AIRQUEST EI, which accounts for the high SO_2 difference between the two emission inventories and some of the CO differences. CO, in general, was higher in all categories (point, area, biogenic) in the NW-AIRQUEST EI than in the NET96 EI.

The remaining large difference between the emission inventories was the NH_3 emission category. NH_3 emissions were much higher in the NET96 EI than in the NW-AIRQUEST EI. Large uncertainties exist in the current state-of-the-knowledge for estimating ammonia emissions. The major sources of NH_3 in the NET96 are animal husbandry operations and fertilizer applications. Seasonal profiles were applied to these source categories with the net effect that 37% of the annual NH_3 emissions occurred during the summer months. For the NW-AIRQUEST EI, NH_3 fluxes reported for livestock by the European Environment Information and Observation Network (EIONET, http://eionet.eea.eu.int/aegb/cap10/b1050.htm) were applied without seasonal adjustments. Ammonia fluxes were also estimated from several agricultural landuse categories. Thus, two very different methods were used to arrive at NH_3 emission estimates. These estimates differ by almost an order of magnitude.

2.3 Initial and Boundary Conditions, Model Spin-Up. Initial and boundary conditions for the gas-phase species were based upon the research of Barna et al. (*2*) and Jiang (*23*). For the aerosol species of SO_4, NH_4, NO_3, elemental carbon, and aerosol water content, clean marine air values were applied from Huebert et al. (*24*) and from studies conducted by McInnes et al. (*25*) and Quinn et al. (*26*) at Cheeka Peak in Washington State. Both the NET96 and the NW-AIRQUEST emission inventory simulations utilize the same gas-phase initial and boundary conditions. The NET96 simulation was run without the benefit of the aerosol species initial and boundary conditions because they were derived as part of the NW-AIRQUEST effort.

The first two forecast days (July 1 and 2) were run twice and not used in the analysis to give a 4-day model spin-up period. This was necessary to remove the effects of initial conditions from the model solution.

3. Aerosol and Ozone Behavior for July 3−15, 1996

Contour plots of 1-hr concentrations of total $PM_{2.5}$, reconstructed β_{ext}, total inorganic aerosols ($SO_4 + NO_3 + NH_4$), and OC across the PNW domain for the NW-AIRQUEST EI solution and NET96 EI solution, are shown in Figure 2 for July 14, 1996 at 7 a.m. PDT, a time when $PM_{2.5}$ concentration maximums occurred. The I-5 corridor is the most heavily urbanized region of the domain, and high aerosol levels occurred downwind along the western crest of the Cascade Mountains, then were advected eastward over the mountains to impact Class I wilderness areas such as Mount Rainier, Mount Adams, and Mount Hood and through the Columbia River Gorge, a protected scenic area. High $PM_{2.5}$ and OC concentrations occurred in central Idaho and impacted the Selway-Bitterroot and Sawtooth Class I wilderness areas. Contour plots of ozone concentration, shown in Figure 3 for the afternoon of July 14, indicate that elevated ozone concentrations were mostly confined to the I-5 corridor from

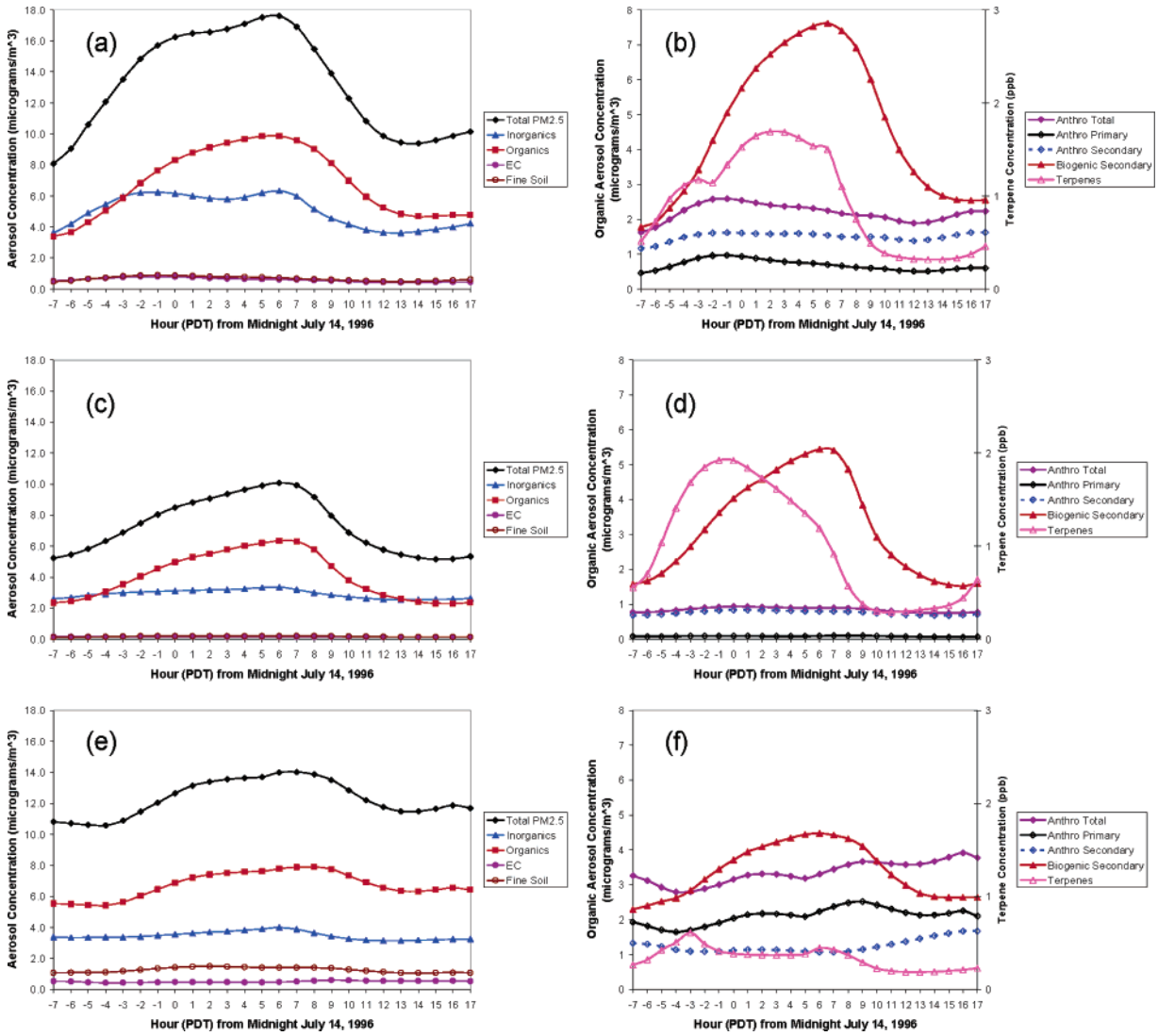

FIGURE 4. One-hour regional average concentrations for the 24-hour period from 5 p.m. PDT July 14, 1996 to 5 p.m. PDT July 15, 1996: (a) aerosol contributions to total $PM_{2.5}$ for the Columbia River Gorge, (b) organic aerosol contributions to total OC for the Columbia River Gorge, (c) aerosol contributions to total $PM_{2.5}$ for Central Idaho, (d) organic aerosol contributions to total OC for the Central Idaho, (e) aerosol contributions to total $PM_{2.5}$ for the Olympics/Puget Sound, and (f) organic aerosol contributions to total OC for the Olympics/Puget Sound.

Vancouver, British Columbia to the California border. Maximum predicted ozone concentrations exceeded 100 ppb downwind of both the Seattle and Portland urban areas.

In the NW-AIRQUEST EI solution (Figure 2a), the $PM_{2.5}$ concentrations were below 20 $\mu g/m^3$ for much of the period, then concentrations increased to approximately 35 $\mu g/m^3$ toward the end of the modeled period in the Columbia River Gorge region, Central Idaho, and the north slope of the Olympic Mountains in the Puget Sound region. The results for the NET96 EI solution were similar in trend to the NW-AIRQUEST EI solution, but $PM_{2.5}$ concentrations were significantly lower with concentrations mostly below 10 $\mu g/m^3$ east of the Cascade Mountains. West of the Cascade Mountains, in the NET96 EI solution, the $PM_{2.5}$ concentrations were mostly below 20 $\mu g/m^3$ with the exception of the Portland region where concentrations reached 45 $\mu g/m^3$.

Light extinction followed a similar pattern as shown in Figure 2c and d for the NW-AIRQUEST and NET96 EI solutions, respectively. Again, most of the impacts in the NET96 EI solution were in western Oregon and Washington whereas the NW-AIRQUEST EI solution also predicted visibility impairment in eastern Oregon and Washington and Idaho. The NW-AIRQUEST EI solution showed visibility degradation in Western Washington and Oregon, and Central Idaho. Measurements at the Mount Rainier and Columbia River Gorge IMPROVE sites registered the largest visibility impacts with extinction coefficients in the range of moderate degradation.

Contour plots of the inorganic aerosol ($SO_4 + NO_3 + NH_4$) contribution to total $PM_{2.5}$ are shown in Figure 2e and f. Inorganic aerosols contributed up to 8 $\mu g/m^3$ to the total $PM_{2.5}$ concentration. This contribution mostly impacted the states of Oregon and Washington west of the Cascade Mountains with some advection through the Columbia River Gorge and over the Cascades into the Columbia Plateau area. This urban effect is much more pronounced in the NET96 EI solution than in the NW-AIRQUEST solution, where Portland, Oregon is a regional hot spot with inorganic aerosol concentrations greater than 15 $\mu g/m^3$.

Results in Figure 4 illustrate the regional diurnal pattern of $PM_{2.5}$ and the individual aerosol species that contribute to $PM_{2.5}$ for three regions of the domain: the Columbia River Gorge (CRG), the Olympics/Puget Sound (OPS), and Central Idaho (CI). These regions were selected because they exhibited higher $PM_{2.5}$ concentration and corresponding visibility degradation, and had either Class I wilderness areas

TABLE 3. Ratio of Contribution of Inorganic Aerosols, Organic Aerosols, Elemental Carbon, Fine Soil, and Other Coarse Mass to Total $PM_{2.5}$, and Ratio of Anthropogenic OC and Biogenic OC to Total OC[a]

	Olympics/ Puget Sound	Columbia River Gorge	Central Idaho
inorganic/$PM_{2.5}$	0.36	0.41	0.40
OC/$PM_{2.5}$	0.44	0.46	0.55
EC/$PM_{2.5}$	0.05	0.06	0.02
finesoil/$PM_{2.5}$	0.12	0.06	0.02
other/$PM_{2.5}$	0.03	0.01	<0.01
anthropogenicOC/OC	0.51	0.35	0.20
biogenicOC/OC	0.49	0.65	0.80

[a] The other coarse mass contribution is from tails of the coarse mode unspecified anthropogenic mass and coarse model soil-derived mass distributions in the $PM_{2.5}$ range.

(such as Central Idaho), locations of scenic vistas (such as the Columbia River Gorge), or both urban and scenic vistas combined (such as the Olympics/Puget Sound). All three regions contain at least one IMPROVE station as shown in Figure 1. The NW-AIRQUEST EI solution was used in this analysis and the period from 5 p.m. PDT July14, 1996 to 5 p.m. PDT July 15, 1996 was selected because peak or near-peak concentrations were predicted in all three regions. In all three regions, $PM_{2.5}$ concentrations grew overnight, peaked at approximately 6−7 a.m., then decreased during the daytime hours following the trend of organic aerosol growth and decay. Little diurnal variation in inorganic (SO_4 + NO_3 + NH_4 + aerosol water content) aerosol concentrations was discernible in any of the three regions. Table 3 gives the ratio contribution of inorganic aerosols, organic aerosols, elemental carbon, and fine soil to total $PM_{2.5}$, and the ratio of anthropogenic OC and biogenic OC to total OC. In all three regions organic carbon was the largest contributor to total $PM_{2.5}$ with fractional contributions ranging from 0.44 for OPS to 0.55 for CI. Inorganic aerosols were the second largest contributor with fractional contributions ranging from 0.36 for OPS to 0.41 for CRG. The influence of elemental carbon and fine soil on total $PM_{2.5}$ was relatively small for all three domains with ratios of 0.02 for CI to 0.12 (fine soil) for OPS. All three regions tended to over-predict total $PM_{2.5}$ when compared with the IMPROVE measured results, however the OC/$PM_{2.5}$ ratios were similar for predicted and observed concentrations at PUSO and CORI where OC measurements were available.

Investigation of the contributions to total OC yields insight into the sources and chemistry affecting each of the three regions. Figures 4b, d, and f show the contributions of anthropogenic OC (primary and secondary) to total OC and the contribution of biogenic OC to total OC. In the Olympics/Puget Sound region, approximately half the OC is biogenic in origin and half is anthropogenic in origin. Of the anthropogenic OC, approximately $^2/_3$ is primary and $^1/_3$ is secondary. This region exhibits the greatest anthropogenic OC concentrations of the three regions. In the Columbia River Gorge region, 65% of the total OC is biogenic in origin and 35% is anthropogenic in origin. Of the anthropogenic portion, secondary production dominates over primary emissions, although the secondary production is very similar to that in OPS. In Central Idaho, the anthropogenic contribution to total OC is only 20% and is mostly secondary in nature; this fits with the fact that there are few primary anthropogenic sources of OC in the area and that chemical reaction of VOCs along the transport path is the primary source of anthropogenic OC.

The biogenic contribution to organic aerosol concentration is directly dependent upon terpene concentrations and the oxidizing capacity associated with OH, NO_3, and O_3 concentrations. Terpene concentrations, shown in Figure 4, peak in the late evening and early morning hours as emissions continue through the night and atmosphere becomes more stable. The relationship of terpene concentrations to biogenic OC formation is linear in the CMAQ aerosol module, but dependent upon the amount of terpenes reacted, which is dependent on the concentration of available radicals. Thus, the three regions exhibit very different ratios of terpene peak concentrations to biogenic OC peak concentrations. The ratios of peak biogenic OC concentration to peak terpene concentration are 2.9 for central Idaho, 4.6 for the Columbia River Gorge, and 7.3 for the Olympics/Puget Sound. The CRG and CI regions have similar terpene concentrations, but the CRG region has greater biogenic OC concentrations. The OPS has the greatest oxidizing capacity of the three regions, and generates the most biogenic OC for the amount of terpenes present. Thus, it is the combination of anthropogenic sources with biogenic sources that results in higher concentrations of biogenic OC, not the presence of terpenes alone—results similar to those described by Pun et al. (*13*) for the eastern United States.

The CRG and OPS regions were both predicted to experience high ozone concentrations at 5 p.m. PDT July 14, 1996, with ranges of 61−183 and 46−172 ppb, respectively. The CI region experienced predicted O_3 concentrations in the range of 45−93 ppb during the same period. At night ozone concentrations were reduced to 35−85 ppb in the CRG region, 30−60 ppb in the OPS region, and 30−45 ppb in the CI region. The elevated ozone levels and availability of nighttime NO_3 allowed for reactions with terpenes to generate secondary OC. This illustrates the complex interaction of biogenic and anthropogenic VOCs and the interaction of ozone and aerosol chemistry.

4. Model Performance Results

Model performance was analyzed for the 13-day period of July 3−15, 1996 in terms of aerosol and ozone concentrations. July 13 and 14, 1996 were days when measured ozone concentrations exceeded or nearly exceeded the 1-hr National Ambient Air Quality Standards (NAAQS) limit of 120 ppb downwind of Seattle and Portland. The maximum measured visibility impairment (β_{ext} = 76 Mm^{-1}) also occurred on Sunday July 14, 1996 at the Mount Rainier IMPROVE site, a rural site located downwind of the Seattle urban area and the I-5 corridor. This level of impact is indicative of severe impairment.

4.1 Particulate Matter and Visibility Results. Evaluation of model performance for total $PM_{2.5}$, the SO_4, NO_3, OC, EC, and SOIL aerosol components, and the β_{ext} and deciview visibility parameters was accomplished by comparing model results against data at 12 IMPROVE stations. Model predictions for $PM_{2.5}$, PM_1, and NH_4 were also compared with measured data from the Spokane Health Effects (SHE) site (*27*). Figure 1 shows the locations of these monitoring sites. The 24-hr average samples taken twice weekly at the IMPROVE sites give 4 data points per station for this analysis. At the SHE site, 1-hr average $PM_{2.5}$ and PM_1 observations and 24-hr averaged NH4 observations were available. The SHE site was located in eastern Washington State and was the only site where NH_4 was measured. The PMx software (*28*, *29*) was used to postprocess the CMAQ output to obtain aerodynamic size resolution concentrations (e.g., PM_1 and $PM_{2.5}$).

Table 4 contains a summary of the normalized mean bias (NMB) and normalized mean error (NME) calculated for the aerosol and visibility parameters at the IMPROVE and SHE sites. Equations 1 and 2 were used to calculate the NMB and NME, respectively, because low concentrations were measured at many of the sites, which can

TABLE 4. Statistical Comparison for Mean Normalized Bias (NMB) and Mean Normalized Error (NME) of the CMAQ NET96 EI Solution and the CMAQ NW-AIRQUEST EI Solution with the 12 IMPROVE Sites (Combined) for $PM_{2.5}$, SO_4, NO_3, OC, EC, SOIL, β_{ext} and Deciview (dv) and with the Spokane Health Effects (SHE) Site for $PM_{2.5}$, PM_1, and NH_4

species	data source	average ($\mu g/m^3$)	no. of observations (averaging period)	NMB (%)	NME (%)
$PM_{2.5}$	IMPROVE	5.5	48 (24-hr)		
	NET96	4.4		−20	52
	NW-AIRQUEST	6.4		16	38
$PM_{2.5}$	SHE	9.8	277 (1-hr)		
	NET96	10		3	38
	NW-AIRQUEST	7.2		−27	34
PM_1	SHE	9.0	237 (1-hr)		
	NET96	8.5		2	48
	NW-AIRQUEST	5.5		−35	47
SO_4	IMPROVE	1.0	28 (24-hr)		
	NET96	0.42		−60	68
	NW-AIRQUEST	1.4		36	68
NO_3	IMPROVE	0.30	28 (24-hr)		
	NET96	0.36		20	107
	NW-AIRQUEST	0.10		−67	73
NH_4	SHE	0.16	11 (24-hr)		
	NET96	0.34		124	139
	NW-AIRQUEST	0.43		170	170
OC	IMPROVE	2.4	26 (24-hr)		
	NET96	2.0		−17	35
	NW-AIRQUEST	3.0		32	49
EC	IMPROVE	0.38	26 (24-hr)		
	NET96	0.61		63	93
	NW-AIRQUEST	0.69		97	104
fine soil	IMPROVE	0.68	48 (24-hr)		
	NET96	0.98		44	111
	NW-AIRQUEST	0.29		−57	71
β_{ext}	IMPROVE	38 *(1/Mm)*	22 (24-hr)		
	NET96	30 *(1/Mm)*		−22	30
	NW-AIRQUEST	39 *(1/Mm)*		1	22
dv	IMPROVE	13	22 (24-hr)		
	NET96	10		−21	27
	NW-AIRQUEST	13		3	18

cause unreasonably high biases and errors (*14*).

$$NMB = \frac{\sum_{i=1}^{N}(c_i^p - c_i^o)}{\sum_{i=1}^{N} c_i^o} \times 100\% \quad (1)$$

$$NME = \frac{\sum_{i=1}^{N}|c_i^p - c_i^o|}{\sum_{i=1}^{N} c_i^o} \times 100\% \quad (2)$$

C_i^p is the model-predicted concentration for station observation i, C_i^o is the observed concentration for station observation i, and N is the number of station observations during the 13-day analysis period. Fractional bias (FB) and fractional error (FE) are another means of evaluating model performance that allows for less stringent performance goals on less abundant species. The fractional bias and fractional error bounds are calculated by

$$FB_{bound} \pm 170e^{-C_o/0.5\mu g/m^3} + 30 \quad (3)$$

$$FE_{bound} \leq 150e^{-C_o/0.75\mu g/m^3} + 50 \quad (4)$$

where C_o is the observed concentration. Then the FB and FE for each aerosol component are calculated by

$$FB = \frac{1}{N}\sum_{i=1}^{N}\frac{(C_i^p - C_i^o)}{\left(\frac{C_i^p + C_i^o}{2}\right)} \quad (5)$$

$$FE = \frac{1}{N}\sum_{i=1}^{N}\frac{|C_i^p - C_i^o|}{\left(\frac{C_i^p + C_i^o}{2}\right)} \quad (6)$$

Boylan and colleagues (*30*), following observations by Seigneur (*31*), recommended (1) that current PM models should achieve normalized errors of 50% or less for $PM_{2.5}$ and sulfate; (2) that for abundant species the FE should be less than or equal to 50% and FB should be less than or equal to 30%; and (3) less abundant species should fall within the boundary curves given by eqs 3 and 4 above.

The CMAQ reconstructed extinction coefficient was used to compare with the extinction coefficient calculated at the IMPROVE sites. CMAQ does not include coarse mass (CM) in its reconstructed extinction coefficient calculation, therefore the CM contribution was removed from the IMPROVE

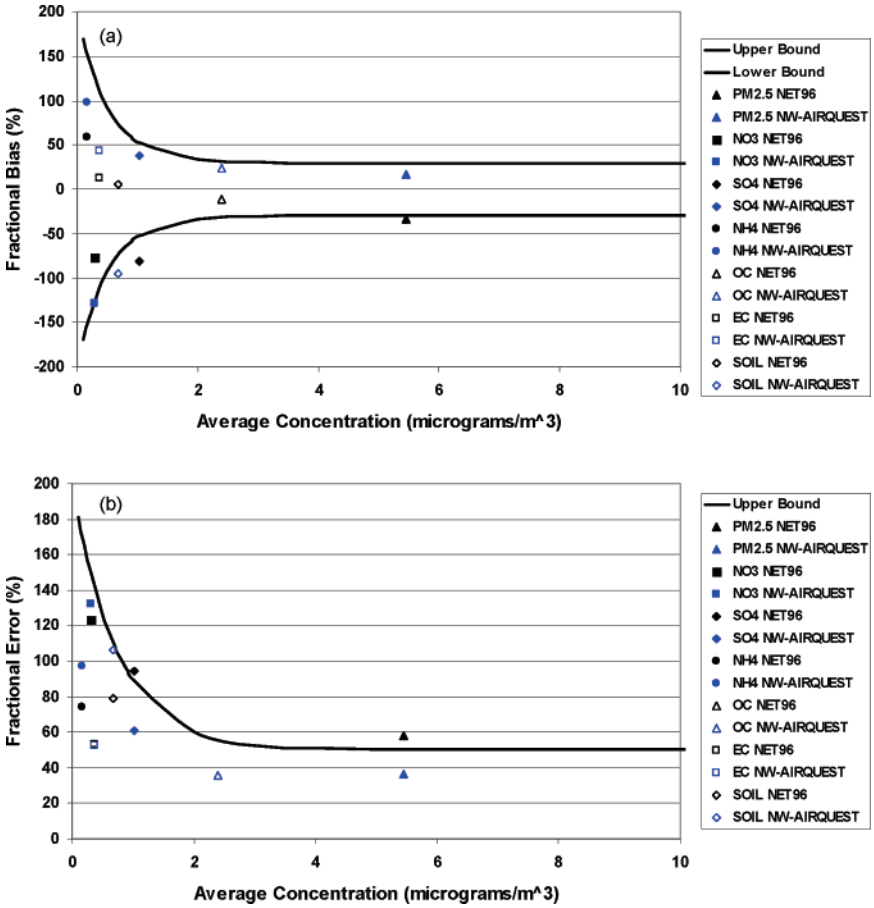

FIGURE 5. (a) Fractional bias and (b) fractional error for the NET96 and NW-AIRQUEST EI solutions versus average observed aerosol species concentration across the 12 IMPROVE measurement sites. NH_4 results are from the SHE site.

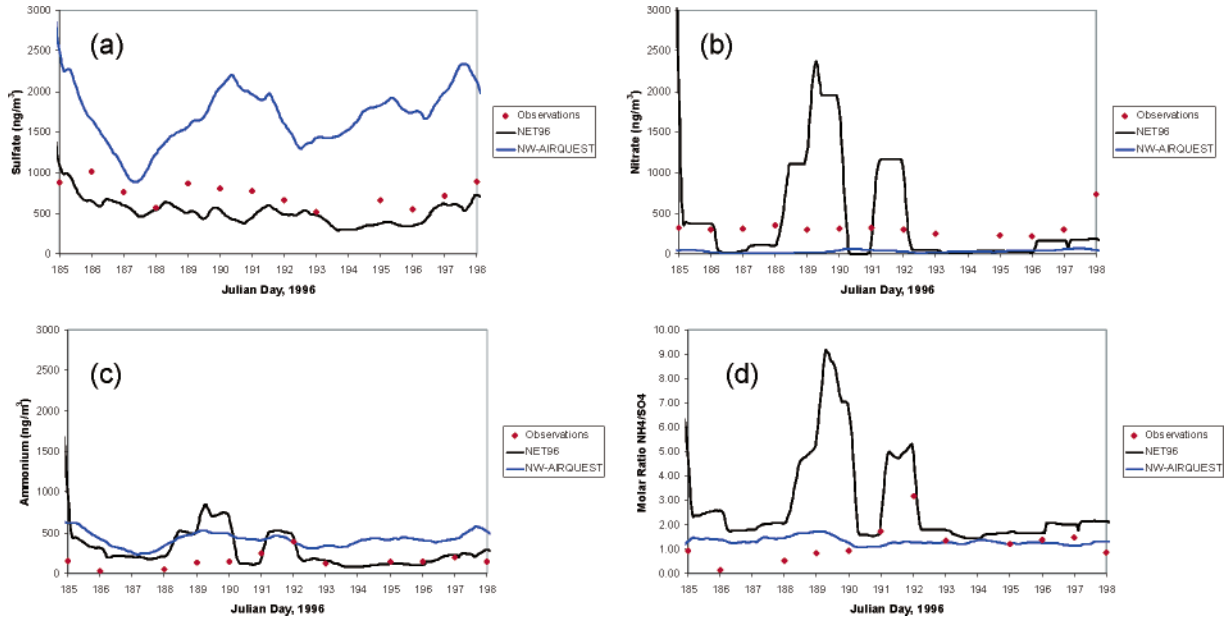

FIGURE 6. Time series beginning July 3, 1996 of model predictions from the NET96 and NW-AIRQUEST EI solutions and observations at the Spokane Health Effects (SHE) site for (a) sulfate, (b) nitrate, (c) ammonium, and (d) the ratio of total ammonium ($TNH_4 = NH_3 + NH_4$) to sulfate (TNH_4/SO_4).

measurements as well. Furthermore, for comparison with the visibility scale provided by Pitchford and Bachman (personal communication), Rayleigh scattering was included in the β_{ext} calculations. Overall, the results in Table 4 and Figure 5 show the two EI simulations tend to bracket the average observed PM parameters and that errors calculated for the model results were within acceptable bounds. The NW-AIRQUEST solution performed well, predicting β_{ext} with a NMB of 1% and NME of 22%, while the NET96 solution tended to under-predict β_{ext} with a NMB of −21%. Deciview results were very similar. Figure 5a and b show the FB and FE for the two EI solutions. The NW-AIRQUEST EI performed

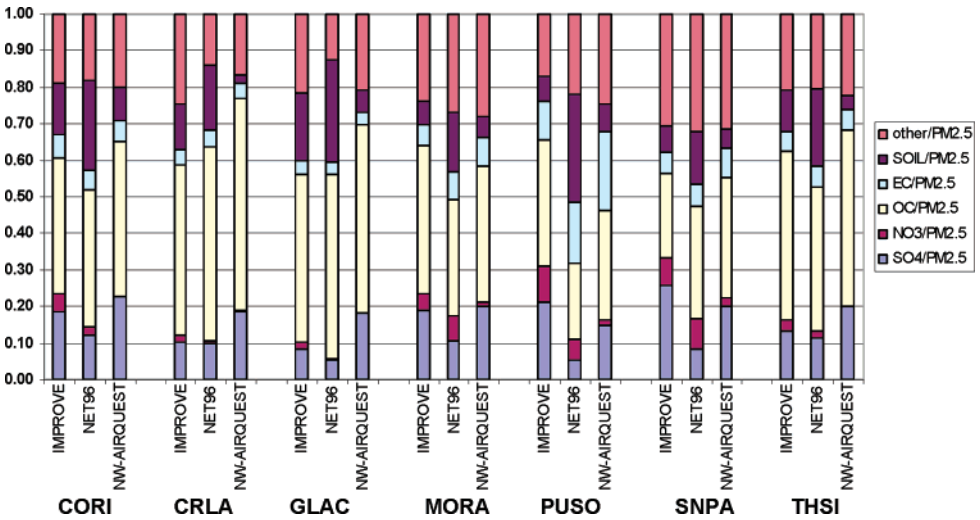

FIGURE 7. Ratio of contribution of each aerosol component to total aerosol mass at the 7 IMPROVES sites with data available for all aerosol components.

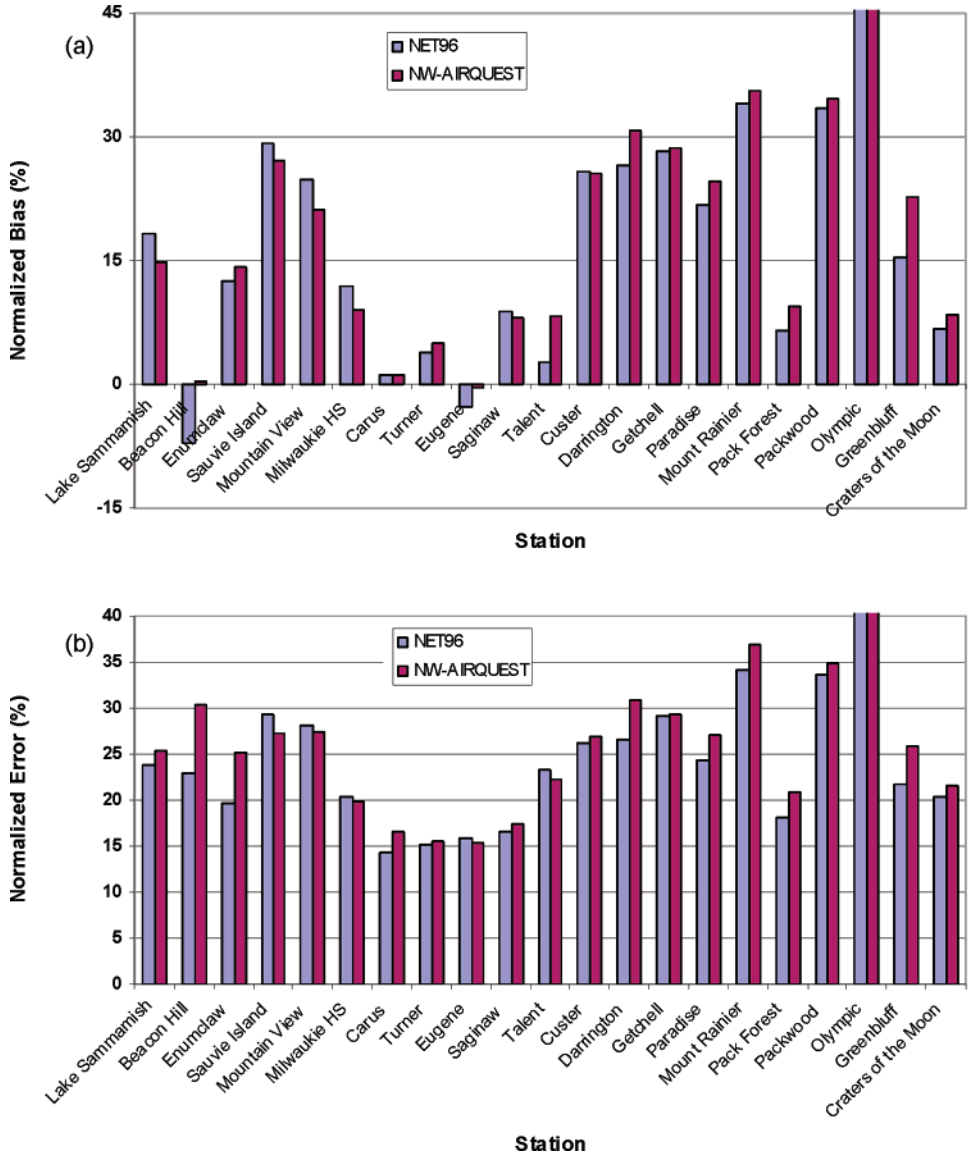

FIGURE 8. (a) Mean bias and (b) mean error for the NET96 and NW-AIRQUEST EI solutions at the 21 ozone measurement stations. The first 11 stations are urban sites located in a north−south line from Seattle to south of Portland, Oregon. The next 7 sites are semi-rural measurement sites located in a north−south line. The last three sites are remote sites at Olympic National Park (the most westward observation station), Greenbluff (eastern Washington), and Craters of the Moon (southern Idaho).

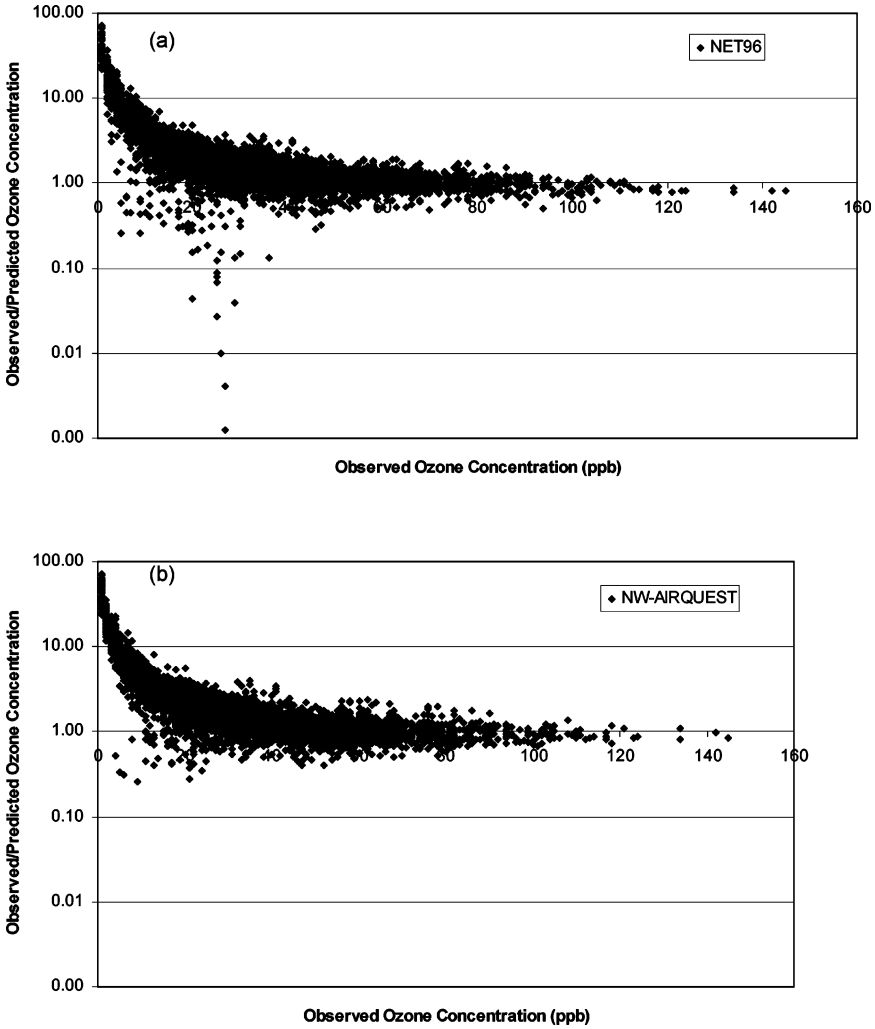

FIGURE 9. Ratio of observed to predicted ozone concentration versus observed ozone concentration for (a) the NET96 EI solution and (b) the NW-AIRQUEST EI solution.

well with all aerosol components falling within the bounds except for SOIL which was under-predicted. Organic carbon is the largest contributor to total aerosol concentration in the PNW and while performing well within error bounds, the NW-AIRQUEST solution tended to over-predict concentrations which could be due to the BEIS3 emission factors being too high as indicated by Pressley et al. (*22*) and/or due to errors in extrapolating organic mass from organic carbon measurements as suggested by Andrews (*32*).

CMAQ models inorganic aerosol formation based on the ratio of total NH_4 ($TNH_4 = NH_4 + NH_3$) to SO_4 (TNH_4/SO_4), temperature, and relative humidity. If the ratio is less than two, then all NH_4 reacts with SO_4 allowing for little NO_3 formation. Figure 6 shows time series plots of SO_4, NO_3, NH_4, and TNH_4/SO_4 at the SHE site. Comparing inorganic aerosol concentrations measured at the SHE site with the modeled results, there is better agreement with the measurements when using the NET96 EI than the NW-AIRQUEST EI. When using the NW-AIRQUEST EI, the modeled TNH_4/SO_4 ratio was less than 2 for the entire period, and, thus, NO_3 formation was prohibited. This is reflected in the consistent positive bias of SO_4 and negative bias of NO_3 at this site throughout the period in the NW-AIRQUEST solution. Coupling this condition with consistent over-prediction of NH_4 and SO_4 suggests that the NW-AIRQUEST solution may be over-estimating SO_2 emissions in eastern Washington. When using the NET96 EI, CMAQ over-predicted the TNH_4/SO_4 ratio at the beginning of the modeling period. Under this NH_4-rich condition, all available SO_4 goes into aerosol phase with NH_4 available for NO_3 aerosol formation also. This is evident with periods of positive bias in nitrate at the site. The first peak of the TNH_4/SO_4 ratio corresponds to the peak nitrate formation. During the second half of the modeling period, the predicted TNH_4/SO_4 ratio follows closely with the observed data at the SHE site. The better performance in modeling the TNH_4/SO_4 ratio with the NET96 EI reflects in better performance in predicting NH_4 and SO_4 concentrations at this site.

The sensitivity of CMAQ inorganic aerosol to the modeled TNH_4/SO_4 ratio was further investigated by Chen (*33*) who varied total input NH_4 and SO_2 emissions by factors between 0 and 2 for the NW-AIRQUEST simulation. The results showed that total $PM_{2.5}$ is sensitive to changes in NH_3 emissions and insensitive to SO_2 emissions for urban sites with $TNH_4/SO_4 > 2$. Under these ammonia rich and NO_x rich conditions, increases in NH_4 emissions increase the formation of both sulfate and nitrate aerosols in the region. The insensitivity to SO_2 emissions is because decreases in SO_2 emissions release additional NH_4 to the system to allow for formation of nitrate aerosol, thus sulfate concentration reductions are offset by nitrate concentration increases.

Figure 7 presents a bar chart comparing modeled versus observed aerosol concentrations for SO_4, NO_3, OC, EC, SOIL and other aerosol mass at the seven IMPROVE sites with full speciated results. The other aerosol mass is composed of aerosol water content, NH_4, and tails of the coarse-mode soil

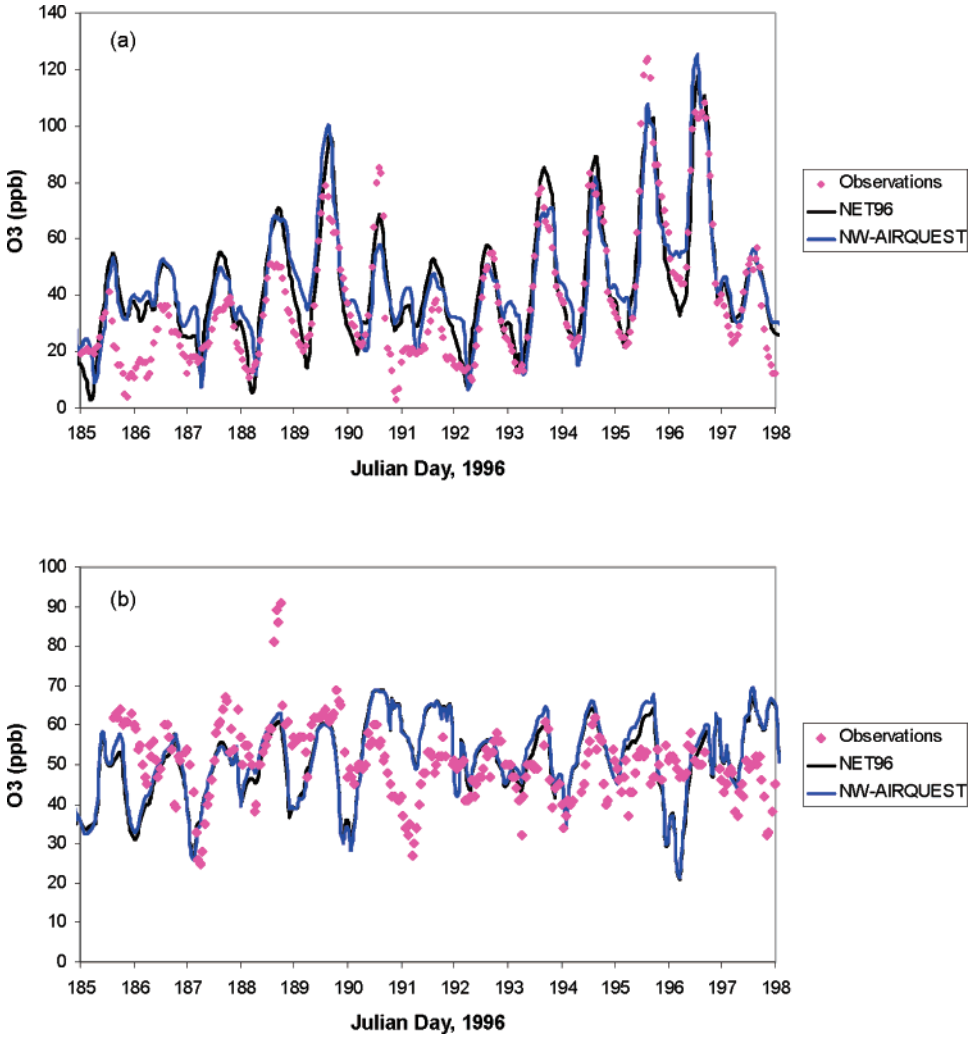

FIGURE 10. Time series beginning July 3, 1996 of predicted ozone concentrations from the NET96 and NW-AIRQUEST solutions and observed ozone concentrations at (a) Carus, Oregon and (b) Craters of the Moon, Idaho.

and unspecified anthropogenic mass distributions. Organic carbon is the largest contributor to total $PM_{2.5}$ with ratios ranging from 21% to 51%. The ratio of OC to $PM_{2.5}$ is similar between the measured IMPROVE data and the two model solutions at each site, despite differences between biogenic emissions in the NET96 and NW-AIRQUEST emission inventories. SO_4 is the second largest constituent comprising $PM_{2.5}$ and greater variations are seen between the observed and modeled data. Adding the SO_4 and NO_3 ratios together gives an indication of which sites are impacted by urban areas. The CORI, MORA, PUSO, and SNPA sites all have $SO_4 + NO_3$ ratios > 24% indicating urban influences, while the CRLA, GLAC, and THIS sites have $SO_4 + NO_3$ ratios < 16% indicating more remote locales.

4.2 Ozone. Figure 3a and b show domain ozone concentrations for July 14, 1996 at 4 p.m. PDT for the NW-AIRQUEST EI solution and the NET96 EI solution, respectively. The two CMAQ solutions performed similarly, as illustrated in Figure 3c, which is a difference plot of the NW-AIRQUEST EI solution and the NET96 EI solution. Differences in the two solutions were below 10 ppb across most of the domain with the exception of the Seattle, WA and Portland, OR areas where the NW-AIRQUEST EI solution predicted higher ozone concentrations than the NET96 EI solution.

Performance in terms of normalized bias (NB) and normalized error (NE) for the two CMAQ solutions versus the observed ozone concentrations at the 21 ozone monitors is shown in Figure 8. Normalized error and normalized bias were calculated by the following:

$$NB = \frac{1}{N}\sum_{i=1}^{N}\left(\frac{C_i^p - C_i^o}{C_i^o}\right) \times 100\% \quad (7)$$

$$NE = \frac{1}{N}\sum_{i=1}^{N}\left|\frac{C_i^p - C_i^o}{C_i^o}\right| \times 100\% \quad (8)$$

The data in Figure 8a and b were calculated using the entire 13-day period, excluding ozone observations less than 40 ppb because normalized quantities can become large when the observations are small (*14*). The two CMAQ EI solutions performed very similarly which is not unexpected given that the VOC/NOX ratios from anthropogenic sources are similar (1.0 for the NW-AIRQUEST solution and 1.2 for the NET96 solution). U.S. EPA's recommended model performance bounds are ±15% for normalized bias and 35% for normalized error (*34*). The NET96 solution had acceptable performance in terms of bias at 11 of the 21 stations and at 9 of the 11 urban stations. Similarly, the NW-AIRQUEST solution had acceptable performance in terms of bias at 11 of the 21 stations and at 10 of the 11 urban stations. Both solutions performed well for normalized error, with the NET96 having NE ≤35% at 20 of the 21 stations, and the NW-AIRQUEST having NE ≤35% at 19 of the 21 stations. These results are

similar to results reported by Barna et al. (*2*) and O'Neill et al. (*35*) using the same subset of urban ozone monitoring stations. Both solutions over-predicted ozone at Olympic National Park, the western-most observational site, located on the north slope of the Olympic Mountains which indicates that the western boundary condition for ozone could be high. Figure 9a and b show the ratio of observed to predicted ozone concentration versus the observed ozone concentration for the NET96 and NW-AIRQUEST EI solutions, respectively. Both figures indicate that the two EI solutions perform quite well for peak ozone concentrations, but tend to over-predict ozone concentrations at the lower observed concentrations. The low ozone concentrations occur at night. The system's poor performance representing nighttime ozone concentrations may be due to errors in nighttime emissions and/or treatment of vertical mixing during stable nighttime conditions. Pleim et al. (*36*) described similar behavior and suggest a modification of the vertical diffusivity as a function of landuse to correct this problem. Analysis involving quantile−quantile plots (not shown) indicate that the two solutions over-predict ozone concentrations by 6−7 ppb at the urban stations. Mahmud (*37*) recently found that a reduction of 5 ppb ozone in the boundary conditions results in a 3 ppb ozone reduction at the ozone monitoring stations in the PNW.

Figure 10a shows predicted and observed ozone concentrations for Carus, OR located downwind of the Portland, OR urban area. Observed ozone concentrations ranged from 2 to 124 ppb during the 13-day period and both simulations captured the observed diurnal variations. Figure 10b shows predicted and observed ozone concentrations for Craters of the Moon, located in rural Southern Idaho. This site shows little diurnal fluctuation in ozone and instead reflects well-mixed transport of ozone, indicating that the eastern and southern boundary conditions are probably appropriate. These example ozone time series plots are similar to urban and rural time series plots presented by Boylan et al. (*14*). At Craters of the Moon, Idaho the average observed ozone concentration for the 13 day period was 51 ppb, and the NET96 and NW-AIRQUEST solutions successfully predicted 51 ppb average ozone and 52 ppb average ozone concentrations, respectively.

Acknowledgments

Many thanks to Alex Guenther, Weimin Jiang, Shelley Pressley, Julia Flaherty, Greg Hernandez, Jeanne Hoadley, Bob Kotchenruther, and Bill Puckett. Thank you also to three anonymous reviewers who helped improve the quality of this paper. This project was funded by the U.S. EPA through the Northwest Regional Modeling Center Models-3/CMAQ Demonstration Project. Computing facilities were provided by the National Center for Atmospheric Research (NCAR) in Boulder, CO and the Center for Multiphase Environmental Research (CMER) at Washington State University. S.O. was funded by a three-year U.S. EPA Science-To-Achieve-Results (STAR) fellowship. Support for this work was also provided through the Boeing Distinguished Professor endowment fund at Washington State University.

Literature Cited

(1) U.S. Environmental Protection Agency. *Science algorithms of the EPA Models-3 Community Multi-scale Air Quality (CMAQ) Modeling System*; EPA/600/R-99/030; U.S. EPA: Washington, DC, 1999.

(2) Barna, M. G.; Lamb, B. K.; O'Neill, S. M.; Westberg, H.; Figueroa-Kaminsky, C.; Otterson, S.; Bowman, C.; DeMay, J. Modeling ozone formation and transport in the cascadia region of the Pacific Northwest. *J. Appl. Meteorol.* **2000**, *39*, 349−366.

(3) Barna, M. G.; Lamb, B. K. Improving ozone modeling in regions of complex terrain using observational nudging in a prognostic meteorological model. *Atmos. Environ*. **2000**, *34*, 4889−4906.

(4) Barna, M. G.; Lamb, B. K.; Westberg, H. Modeling the effects of VOC/NO_x emissions on ozone synthesis in the Cascadia airshed of the Pacific Northwest. *J. Air Waste Manage. Assoc*. **2001**, *51*, 1021−1034.

(5) Jiang, G.; Lamb, B. K.; Westberg, H. Using back trajectories and process analysis to investigate photochemical ozone production in the Puget Sound region. *Atmos. Environ*. **2003**, *37*, 1489−1502.

(6) Malm, W. C.; Sisler, J. F.; Huffman, D.; Eldred, R. A.; Cahill, T. A. Spatial and seasonal trends in particle concentration and optical extinction in the United States. *J. Geophys. Res*. **1994**, *99*, D1, 1347−1370.

(7) Malm, W. C.; Day, D. E. Optical properties of aerosols at Grand Canyon National Park. *Atmos. Environ.* **2000**, *34*, 3373−3391.

(8) U.S. Environmental Protection Agency. *National Air Pollutant Emission Trends, 1900−1998*; EPA-454/R-00-002; U.S. EPA: Washington, DC, 2000.

(9) Pierce, T.; Geron, C.; Bender, L.; Dennis, R.; Tonnesen, G.; Guenther, A. Influence of increased isoprene emissions on regional ozone modeling. *J. Geophys. Res*. **1998**, *103*, D19, 25611.

(10) Guenther, A.; Geron, C.; Pierce, T.; Lamb, B.; Harley, P.; Fall, R. Natural emissions of nonmethane volatile organic compounds, carbon monoxide, and oxides of nitrogen from North America. *Atmos. Environ*. **2000**, *34*, 2205−2230.

(11) Geron, C. D.; Guenther, A. B.; Pierce, T. E. An improved model for estimating emissions of volatile organic compounds from forests in the eastern United States. *J. Geophys. Res*. **1994**, *99*, 12773−12791.

(12) Pierce, T. E.; Geron, C. D.; Bender, L.; Dennis, R.; Tonnesen G.; Guenther, A. Influence of increased isoprene emissions on regional ozone modeling. *J. Geophys. Res*. **1998**, *103*, 25611−25629.

(13) Pun, B. K.; Wu, S. Y.; Seigneur, C. Contribution of Biogenic Emissions to the Formation of Ozone and Particulate Matter in the Eastern United States. *Environ. Sci. Technol*. **2002**, *36*, 3586−3596.

(14) Boylan, J. W.; Odman, M. T.; Wilkinson, J. G.; Russell, A. G.; Doty, K. G.; Norris, W. B.; McNider, R. T. Development of a comprehensive, multiscale "one-atmosphere" modeling system: application to the Southern Appalachian Mountains. *Atmos. Environ.* **2002**, *36*, 3721−3734.

(15) Qin, Y.; Tonnesen, G. S.; Wang, Z. Weekend/weekday differences of ozone, NO_x, CO, VOCs, PM_{10} and the light scatter during ozone season in southern California. *Atmos. Environ.* **2004**, *38*, 3069−3087.

(16) Grell, A. G.; Dudhia, J.; Stauffer, D. R. *A description of the fifth-generation Penn State/NCAR Mesoscale Model (MM5)*; NCAR Technical Note NCAR/TN-398+STR; The National Center for Atmospheric Research: Boulder, CO, 1994.

(17) Mass, C. F.; Ovens, D.; Westrick, K.; Colle, B. A. Does increasing horizontal resolution produce more skillful forecasts? The results of two years of real-time numerical weather prediction over the Pacific Northwest. *Bull. Am. Meteorol. Soc.* **2002**, *83* (3), 407−431.

(18) Houyoux, M.; Vukovich, J. *Updates to the Sparse Matrix Operator Kernel Emissions (SMOKE) modeling system and integration with Models-3*; Presented at the Air & Waste Management Association Conference, Emissions Inventory: Regional strategies for the future; Raleigh, NC, October, 1999.

(19) Washington State Department of Ecology (WA DOE), Oregon Department of Environmental Quality, Idaho Department of Environmental Quality, EPA Region 10, Washington State University, University of Washington, Environment Canada. *The Regional Technical Center Demonstration Project Summary Report, 2002*; Washington State Department of Ecology: Olympia, WA, 2002.

(20) Kinee, E.; Geron, C.; Pierce, T. Land Use Inventory for Estimating Biogenic Ozone Precursor Emissions. *Ecol. Appl.* **1997**, *7* (1), 46−58.

(21) Pierce, T.; Geron, C.; Pouliot, G.; Kinnee, E.; Vukovich, J. Integration of the biogenic emissions inventory system (BEIS3) into the community multiscale air quality modeling system. 12th Joint Conference on the Applications of Air Pollution Meteorology with the Air and Waste Management Association; American Meteorological Society: Boston, MA, 2002.

(22) Pressley, S.; Lamb, B.; Westberg, H.; Guenther, A.; Chen, J.; Allwine, E. Monoterpene emissions from a Pacific Northwest old-growth forest and impact on regional biogenic VOC emission estimates. *Atmos. Environ.* **2004**, *38*, 3089−3098.

(23) Jiang, G. Ph.D. Thesis, Washington State University, Department of Chemistry, Pullman, WA, 2001.

(24) Heubert, B. J.; Howell, S. G.; Zhuang, L.; Heath, J. A.; Litchy, M. R.; Wylie, D. J.; Kreidler-Moss, J. L.; Coppicus, S.; Pfeiffer, J. E. Filter and impactor measurements of anions and cations during the First Aerosol Characterization Experiment (ACE 1). *J. Geophys. Res.* **1998**, *103*, D13, 16493−16509.
(25) McInnes, L. M.; Quinn, P. K.; Covert, D. S.; Anderson, T. L. Gravimetric analysis, ionic composition, and associated water mass of the marine aerosol. *Atmos. Environ.* **1996**, *30* (6), 869−884.
(26) Quinn, P. K.; Marshall, S. F.; Bates, T. S.; Covert, D. S.; Kapustin, V. N. Comparison of measured and calculated aerosol properties relevant to the direct radiative forcing of tropospheric sulfate aerosol on climate. *J. Geophys. Res.* **1995**, *100*, D5, 8977−8991.
(27) Norris, G. Ph.D. Thesis, University of Washington, Department of Civil and Environmental Engineering, Seattle, WA, 1998.
(28) Jiang, W.; Yin, D. *Development and application of the PMx software package for converting CMAQ modal particulate matter results into size-resolved quantities*; PET-1497-01S; Program of Energy Research and Development, Natural Resources Canada: Ottawa, ON, 2001.
(29) Jiang, W.; Yin, D. Mathematical formulation and consideration for converting CMAQ modal particulate matter results into size-resolved quantities. American Meteorological Society Fourth Conference on Atmospheric Chemistry: Urban, Regional, and Global-Scale Impacts of Air Pollutants, 2002; pp 7−14.
(30) Boylan, J.; Anderson, B.; Wilson, R. Base Case Development (Air Quality and Meteorology). Presentation at the EPA Particulate Matter, Regional Haze, Ozone Modeling Workshop, June, 2003, Santa Fe, NM.
(31) Seigneur, C. Current status of air quality models for particulate matter. *J. Air Waste Manage. Assoc.* **2001**, *51*, 1508−1521.
(32) Andrews, E.; Saxena, P.; Musarra, S.; Hildemann, L. M.; Koutrakis, P.; McMurry, P. H.; Olmez, I.; White, W. H. Concentration and composition of atmospheric aerosols from the 1995 SEAVS experiment and a review of the closure between chemical and gravimetric measurements. *J. Air Waste Manage. Assoc.* **2000**, *50*, 648−664.
(33) Chen, J. C. M. S. thesis, Washington State University, Department of Civil and Environmental Engineering, Pullman, WA, 2002.
(34) U.S. EPA. *Guidance for Regulatory Application of the Urban Airshed Model (UAM)*; Office of Air Quality Planning and Standards, U.S. Environmental Protection Agency: Research Triangle Park, NC, 1991.
(35) O'Neill, S. M.; Lamb, B. K. Inter-comparison of the Community Multi-scale Air Quality (CMAQ) model and CALGRID using Process Analysis. *Environ. Sci. Technol.* **2004**, *39*, 5742−5763.
(36) Pleim, J.; Mathur, R. Diagnostic evaluation, sensitivity analyses, and new development in the Eta/CMAQ air quality forecast system. Paper presented at the 7th Conference on Atmospheric Chemistry organized by the American Meteorological Society, January 10−13, 2005, San Diego, CA.
(37) Mahmud, A. M. S. thesis, Washington State University, Department of Civil and Environmental Engineering, Pullman, WA, 2005.

Received for review October 12, 2004. Revised manuscript received September 28, 2005. Accepted November 4, 2005.

ES048402K